JOURNAL OF THE KOREAN ASTRONOMICAL SOCIETY
37: 179 ~ 184, 2004

DEVELOPMENT OF WIDE-FIELD IMAGING CAMERA FOR ZODIACAL LIGHT OBSERVATION

S. M. KWON[1], S. S. HONG[2], AND K. J. SHIN[3]
[1]Department of Science Education, Kangwon National University, Chunchon, Korea;
E-mail: smkwon@kangwon.ac.kr
[2]Astronomy Program, SEES, Seoul National University, Seoul, Korea;
E-mail: sshong@astroism.snu.ac.kr
[3]Byulmaro Astronomy Observatory, Yeonwol-gun, Korea;
E-mail: moonskill@hanmail.net
(Received December 1, 2004; Accepted December 22, 2004)

ABSTRACT

We have developed a wide-field imaging camera system, called WICZO, to monitor light of the night sky over extended period. Such monitoring is necessary for studying the morphology of interplanetary dust cloud and also the time and spatial variations of airglow emission. The system consists of an electric cooler, a CCD camera with 60% quantum efficiency at 500nm, and a fish-eye lens with 180° field of view. Wide field imaging is highly desired in light of the night sky observations in general, because the zodiacal light and the airglow emission extend over the entire sky. This paper illustrates the design of WICZO, reports the result of its laboratory performance test, and presents the first night sky image, which was taken, under collaboration with Byulmaro Observatory, on top of Mt. Bongrae at Yongweol in January, 2004.

Key words : instrumentation: miscellaneous, interplanetary medium

I. INTRODUCTION

The zodiacal light(ZL) is the sunlight scattered by interplanetary dust particles(IPDs). Since Earth resides within IPD cloud itself, the zodiacal light ought to be seen all over the sky. However, it is very difficult for an Earth bound observer actually to isolate the zodiacal light in the light of the night sky. This is because the observed brightness of the night sky consists of many components other than the zodiacal light. They are resolved bright stars, integrated light of unresolved faint stars, diffuse Galactic light, Earth's airglow emission, and diffusely scattered light of all the extended sources by scatterers in the Earth's atmosphere. To make the isolation task even more difficult they are more-or-less of the same strength. To sort out all these components we are to make a full use of the characteristics in their spatial distributions (Kwon 1990). For example, the distribution of the integrated starlight and diffuse Galactic light are best described in terms of the Galactic coordinates; while the airglow emission is in the system of horizontal coordinates. For the zodiacal light the ecliptic coordinate system is the best choice of course. Therefore, a capability of wide field imaging is a mandate for studying the zodiacal light phenomenon.

Through many previous studies(Kwon & Hong 1998 and references therein.) it is clear that the maximum density plane of the IPD cloud is slightly dis-aligned with respect to the ecliptic plane. Yet, it is unclear where the maximum density plane is exactly located. The dis-alignment brings about small, but meaningful seasonal changes in details of the zodiacal light brightness distribution. It is these seasonal changes that will eventually allow us to locate the maximum density plane of the IPD cloud. Therefore, monitoring is required over at least a full year period.

The IPD cloud is not a featureless object. It has such diverse structures as IRAS dust bands (Low *et al.* 1984; Dermott *et al.* 1984, 1985; Sykes 1988; Ishiguro *et al.* 1999), cometary dust trails (Davies *et al.* 1984, Sykes & Walker 1992, Ishiguro *et al.* 2002), and circumsolar ring of dusts locked in the Earth's mean motion resonance (Reach 1991, Dermott *et al.* 1994). The bands and trails are structures with amplitude of a few percents and in scale of ten arc minutes or less. Combined with these in-homogeneities in the particle density distribution, structures in the IPD scattering phase function seem to have generated, in the ZL brightness distribution, additional fluctuations of 10° ~ 15° periodicity and 10% relative amplitude (Kwon *et al.* 2004). On the other hand, the global distribution of IPDs is a result of long-term perturbations given to the IPD orbits by the solar radiation and major planets. As their names suggest, detail observations of the features will tell us the origin and dynamical evolution of the IPDs in the solar system. These attributes of the IPD cloud complex demand us to make observations of at least a tenth of degree resolution.

The ZL is notoriously faint in high ecliptic latitudes. For example, at latitude 60, its brightness becomes mostly less than one hundred 10th magnitude solar

Corresponding Author: S. M. Kwon

type stars in one square degree, i.e. one 5th magnitude star in $1^\circ \times 1^\circ$ square. To study the small-scale features of a few percents amplitude, therefore, we need high sensitivity and wide dynamic range.

The high sensitivity and imaging capability of Charge Coupled Device (CCD) was believed to meet all these stringent observational requirements of the ZL studies. James *et al.*(1997) demonstrated that a portable, inexpensive system of CCD camera equipped with fish-eye lens can obtain "snapshot" of diffuse faint extended sources like the zodiacal light. Unlike the photometry of point sources, we are not allowed to subtract background brightness, since our interest is in the background itself. Therefore, stability of photometric zero level is an important factor to consider in the zodiacal light photometry, and cooling is definitely necessary for the system.

About three years ago we decided to develop a wide-field, cooled CCD camera system for an exclusive use in the light of the night sky observations. In the early beginning of this year, we finally obtained the night sky image on top of Mt. Bongrae in Yeongwol area. In this paper we will explain the design strategy, report some of the laboratory test results, and present the first image of the zodiacal light cone.

II. DESCRIPTION OF THE SYSTEM

(a) CCD Camera Head

As described in Introduction, the stability of the CCD camera is a critical factor in absolute photometry of zodiacal light. Fluctuations of the CCD chip temperature can cause uncertainties in the zero level and hence degrade the chip sensitivity. We thus have installed an electric cooler in addition to the compact water circulation cooling system. The chip has a huge imaging area (24.6 × 24.6 mm, 1024 × 1024 pixels) and high sensitivity (QE $\sim$ 60% at 550nm). Table 1 summarizes specifications of KAF1001E CCD chip. The measured temperature and its stability are described in Section 3.

TABLE 1
SPECIFICATIONS OF CCD CHIP

Type	Front Illuminated CCD
Format	1024 x 1024 pixels
Pixel scale	24 x 24 micron
Image area	24.6 x 24.6 mm
QE (%)	60 % 550 nm
Peak signal	180k e^-/pixel
Exposure time	1/100 sec

(b) Optics and Mounting

Since observed flux of diffuse source is inversely proportional to square of the camera f-number, we decided to employ a lens unit with f-number as smallest as possible. Another condition is on the camera field of view. To make accurate corrections of the atmospheric extinction, it is necessary to determine the zenith extinction optical depth for each image frame separately (Kwon 1990). To do this we wanted the camera to cover the whole hemisphere in a single frame. Since the sky brightness at the horizon has the ZL information at the smallest solar elongation, we cherish the night sky brightness even at the horizon. Furthermore, to fix the zenith distance dependence of atmospheric diffuse light, it is necessary to know the sky brightness from the zenith all the way to the horizon (Hong *et al.* 1998). To meet all these criteria, we decided to employ a fish-eye lens designed and developed by *Nikon Camera Corporation* in our camera system. The layout of the lens system is illustrated in Figure 1. Its f-number and focal length F are $f/2.8$ and 8.0 mm, respectively. The lens covers the whole 180° hemisphere, which renders a circular image onto the CCD chip.

A set of five filters is built into the rear end of the lens mount. They are the skylight (L1BC), medium yellow (Y48), deep yellow (Y52), orange (O56), and red (R60) filters. We mounted them on a revolving turret, so that they can be quickly moved into place one after another. The central wavelengths of Y48 and Y52 filters are placed in those regions of the electromagnetic spectrum where the Earth's airglow doesn't show any prominent emission lines. Specifications of the optical assembly are summarized in Table 2.

TABLE 2
SPECIFICATIONS OF THE OPTICS

Focal length/Aperature	8 mm f/2.8
Picture angle	180 degrees
Effective picture field	23 mm-diameter
Lens construction	10 elements in 8 groups
Projection formula	Equidistance
Lens mount	Nikon F bayonet mount
Aperature scale	$f/2.8$ $f/22$

Whole lens system is mounted on a 10-mm thick aluminum plate to prevent a load-deflection (Figure 2). The CCD camera is mounted on the same plate, and connected with the lens by a special T-mounting adapter. To align surface of CCD chip perpendicularly to the lens optical axis, we have installed two-adjustable knobs on the mounting plate and ring. This mounting plate is fixed on an NJP equatorial mount made by the *Takahashi Corporation*, which provides a convenient platform for star trackings anywhere in the region with geographic latitude between ±48°. A picture of the fully assembled system is shown in Figure 3.

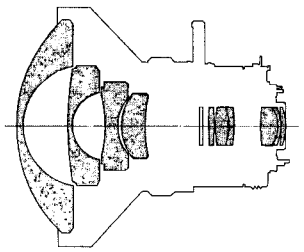

Fig. 1.— The layout of lens, provided by the Nikon Camera Corporation. The optical system is consisted of 10 elements in 8 groups. A filter wheel is located at the rear end of the lens mount. Aperture and focusing rings are equipped for precise exposure.

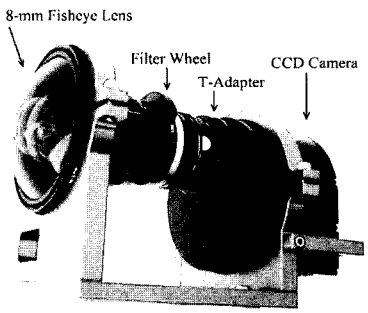

Fig. 2.— Optics and CCD camera of WICZO system.

(c) Operation

The block diagram shown in Figure 4 illustrates how one may operate the WICZO system and control the data acquisition flow. To suppress electric noise, we turned the electric power of the equatorial driving motor off during the test observations. The shutter and temperature of the CCD camera are controlled by a commercial CCD control software called *MaxIm/DL*. The camera and control notebook computer are connected by a generic parallel communication port. The data first obtained in analogue form are converted to digital data inside the CCD camera, and then transferred to the host computer. Although the CCD control software provides 3 modes of sampling rate, we fixed at the lowest transfer speed during the test observations. In this way we tried to reduce the readout noise. The readout noise measured under this configuration is about 16 e^-. It takes $\sim$ 3 minutes for the system to read out the whole frame data.

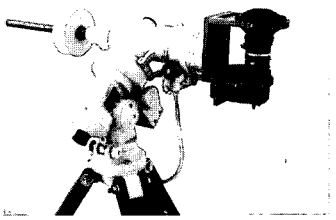

Fig. 3.— Whole view of WICZO.

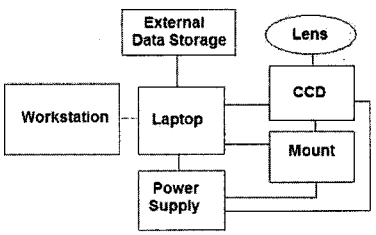

Fig. 4.— Block diagram

III. PERFORMANCE EVALUATION

Before taking the camera system to the observing site, we tested performance of the cooling system in two laboratories, one at Seoul National University and the other Kangwon National University. At both places the chip temperature was monitored under the condition of room temperature, which was about 300 K. In the beginning of the cooling performance test the power was turned off the electric cooler, and the target temperature was set at $-20°$C, which was about 40 degrees below the ambient temperature. We then put the power on, and followed the temperature change. As shown in Figure 5, the temperature drops to the target value in about 5 hours, and remains constant at $-20°$C until the experiment ends. In the laboratory environments the cooling system of WICZO can cool the CCD chip by maximum 50 degrees below the ambient temperature. We performed the same monitoring experiment at the observing site, Mt. Bongrae. We have confirmed that the CCD chip can be cooled down to $-30°$C by our cooling system that is consisted of the electric cooler and the compact water circulator. After stabilizing period, the WICZO cooling system maintains, over the whole observing session, the chip temperature at the target value within rms fluctuation of 0.1 degrees.

By comparing dark frames taken with different exposure times with each other, we estimated the dark current to be less than roughly 0.2 e^-/sec/pixel. With the dark frame obtained for the same exposure time with a given light frame, we examined the stability of photometric zero level. The standard deviation is found to be

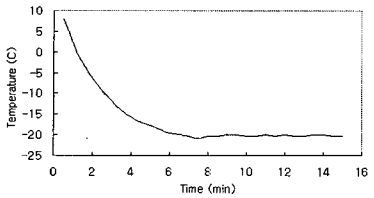

Fig. 5.— Result of cooling experiment

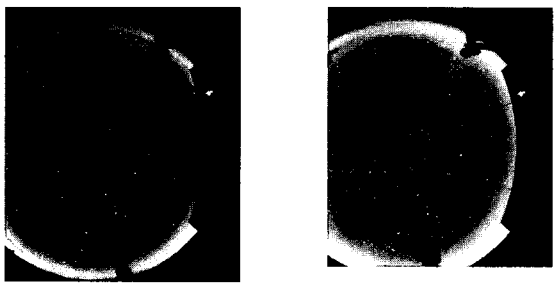

Fig. 6.— A sample image of all-sky monitoring observation with WICZO system. The Milky Way and the morning zodiacal light cone can be easily seen in the frame.

0.37 e^-. The ZL brightness at solar elongation 90° in the ecliptic plane corresponds to 1.1 e^-/sec. Therefore, with 3 minute exposure, the uncertainty of photometric zero level becomes only 0.3% of the zodiacal light brightness.

It was early in January this year that we had WICZO take the first image of night sky. But at that time we could not make a careful performance test. The observations of performance tests were done on 10 nights over the period August 18 through October 31, 2004. In the following analysis, we will use the data set that were obtained with 60 second exposure at 18:13UT on October 12 and with 120 second exposure at 18:52UT on October 13. After each exposure of light frame, we closed the shutter and took a dark frame. A sample of the all-sky images taken in this period is shown in Figure 6.

The circular photographic image produced by the fish-eye lens is an exact reproduction on a flat plane of all the objects encompassed within the 180° hemisphere field. In wide-field imaging observations the geometric calibration should be established for given camera system. With the calibration one may retrieve the celestial coordinates of the objects from their positions in the image. Generally the equidistance projection formula is used in order to accommodate extra-wide view angle within a field of finite size. The zenith distance of any point in the image recorded on a CCD chip is proportional to the distance from the center of the image.

The center of the image corresponds to the zenith in

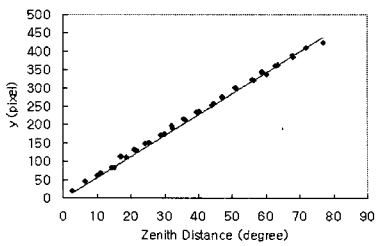

Fig. 7.— Empirical photogrammetry relation for the fish-eye lens

the field of view, and the distance of any point in the image from the center is directly proportional to its angle from the zenith, expressed by the equation, $y = Cz$, where y is the distance of the point from the image center, z is the zenith distance, and C is a constant which we should determine.

In order to fix C, we selected a star in the image, whose position is known in terms of the celestial coordinates. We first calculated the zenith distance of the star at the time of observation, and then measured, in pixel units, linear distance of the star from the center of the image. The same measurement was done for many selected stars from the same CCD image. The resulting distances of all the stars were plotted, in Figure 7, against their zenith distances. A linear least squares fit to the data fixes the constant $C = 5.71$ pixel/deg. As can be seen from the figure, all the stars lie on a single line of fixed slope or very close to it. Since they are distributed more-or-less uniformly over the image frame, the vectors connecting the zenith and the stars point all different directions in the image plane. Yet, all the points draw a single line of fixed slope. This indicates that the projection factor of the WICZO system is independent of direction

The magnitude m of the photometric standard stars in the WICZO photometric system is defined as $m = V + K(B - V)$, where K is the color correction coefficient. To minimize the effect of atmospheric extinction on the standardization, we selected, from the Bright Star Catalogue, those eight standard stars whose zenith distances at the time of observation carried air mass in the range from 1.0 to 1.1. In Figure 8, we have compared instrumental magnitudes of the stars with their standard values. The abscissa means the instrumental magnitude measured by the aperture photometry utility of *MaxIm/DL*, and the ordinate denotes the reference magnitude of the standard stars. It is found that the best-fit value of K is 0.92. The color correction coefficient will be refined further by employing more standard stars.

Laboratory measurements of photon and read-out noises of our WICZO system indicate the 5 sigma level of detection limit to be 2.3 S10(G2V)/pixel/min. Typical brightness of the night sky right after the end of

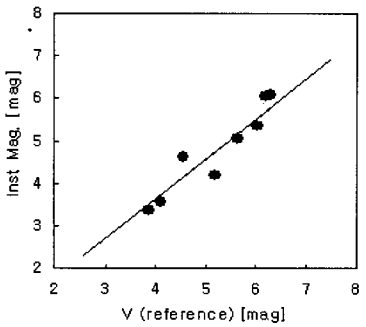

Fig. 8.— Comparison of instrumental magnitude and standard magnitude in WICZO system

TABLE 3
SUMMARY OF THE PERFORMANCE OF WICZO

Read-out noise / time	16 e^-, 60 sec.
Uncertainty of zero level	0.37 e^-
Dark current	<0.2 e^-/sec/pixel
Field-of-view	180-degree circular
Spatial resolution	11.3 arcmin/pixel
Observed ZL intensity at $(\lambda, \beta) = (90, 0)$	$\sim 1.1e^-$/sec

astronomical twilight, for example, is as high as 1500 S10(G2V), which makes the signal-to-noise (S/N) ratio approximately 20. The small-scale structures we saw in the ZL brightness distribution (Kwon *et al.* 2004) show about 10% fluctuations over the smoothed out value of the brightness. The ZL brightness, for example, at solar elongation 90° in the ecliptic plane is 182 S10(G2V). Therefore, the WICZO system would detect such structures with S/N ratio higher than about 4.

IV. SUMMARY AND FUTURE WORK

This paper sets out to investigate the capability of the WICZO system for zodiacal light observations. Results of the performance test done to the system are summarized in Table 3. Although we have managed to suppress the read-out noise, it is still high. The noise resulted in the observed brightness of the zodiacal light is dominated by the read-out noise. On the other hands, photometric zero level is stable enough to map the 2D distribution of the zodiacal light brightness. We may conclude that the WICZO system is a powerful instrument for studying the smooth component of the IPD cloud complex. To make this system useful for the studies of extremely faint and small-scale structures in the complex, means should be found of reducing the read-out noise significantly and improving the spatial resolution substantially. These can be achieved later.

There are still a few problems to solve. Of them flattening is an acute one. Images taken by a wide-field camera generally suffer from strong vignetting, that is, central part of the image frame is brighter than the frame edge. In addition to the vignetting, there ought to be pixel-to-pixel variations in sensitivity. Constructing the flat-frame for correcting them requires the integrating sphere. However, to accommodate the WICZO's huge field-of-view, one needs an integrating sphere with diameter larger than about 2m. This is certainly a formidable task for us. Instead we may have to develop some indirect ways of flattening.

ACKNOWLEDGEMENTS

Authors express special thanks to prof. M. Ueno at Tokyo University for his valuable comments and discussion on the construction of the WICZO system. This research was supported by a Korea Research Foundation grant (KRF-2001-015-DP0609). SSH would like to acknowledge a partial support from the Korea Science and Engineering Foundation via R14-2002-058-01003-0, with which purchasing of the high sensitivity CCD chip was possible.

REFERENCES

Davies, J. K., Green, S. F., Stewart, B. C., Meadows, A. jJ., & Aumann, H. H. 1984, The IRAS fast-moving object search, Nature, 309, 315

Dermott, S. F., Nicholson, P. A., Burns, J. A., & Houck, J. R. 1984, Origin of the solar system dust bands discovered by IRAS, Nature, 312, 505

Dermott, S. F., Nicholson, P. D., Burns, J. A., & Houck, J. R. 1985, An analysis of IRAS' solar system dust bands, in *Properties and Interactions of Interplanetary Dust*, ed. by R. H. Giese, P. Lamy, (D. Reidel:Dordrecht), p.395

Dermott, S. F., Jayaraman, S., Xu, Y. L., Gustafson, B. A. S., & Liou, J. C. 1994, A circumsolar ring of asteroidal dust in resonant lock with the Earth, Nature, 369, 719

Hong, S. S., Kwon, S. M., Park, Y.-S., & Park, C. 1998, Transfer of diffuse astronomical light and airglow in scattering Earth atmosphere, Earth, Planets, and Space, 50, 487

Ishiguro, M., Nakamura, R., Fujii, Y., Morishige, K., Yano, H., Yasuda, H., Yokogawa, S., & Mukai, T. 1999, First detection of visible zodiacal dust bands from ground-based observations, ApJ, 511, 432

Ishiguro, M., Watanabe, J., Usui, F., Tanigawa, T., Kinoshita, D., Suzuki, J., Nakamura, R., Ueno, M., & Mukai, T. 2002, First Detection of an Optical Dust Trail along the Orbit of 22P/Kopff, ApJ, 572, L117

James, J. F., Mukai, T., Watanabe, T., Ishiguro, M., & Nakamura, R. 1997, The morphology and brightness

of the zodiacal llight and gegenschein, MNRAS, 288, 1022

Kwon, S. M. 1990, "A fine resolution study of the zodiacal light distribution", PhD Thesis, Seoul National University

Kwon, S. M. & Hong, S. S. 1998, Three-dimensional infrared models of the interplanetary dust distribution, EP&S, 50, 501

Kwon, S. M., Hong, S. S., & Weinberg, J. L. 2004, An observational model of the zodiacal light brightness distribution, NewA., 10, 91

Low, F. J., Young, E., Beintema, D. A., Gautier, T. N., Beichman, C. A., Aumann, H. H., Gillett, F. C., Neugebauer,G., Boggess, N., & Emerson, J. P. 1984, Infrared cirrus - New components of the extended infrared emission, ApJ, 278, L19-L22

Reach, W. T. 1991, Zodiacal emission. II - Dust near ecliptic, ApJ, 369, 529

Sykes, M. V. 1988, IRAS observations of extended zodiacal structures, ApJ., 334, L55

Sykes, M. V., & Walker, R. G. 1992, Cometary dust trails. I - Survey, Icarus, 95, 180